Int. J. Plant Sci. 155(4):421–436. 1994.

1058-5893/94/5504-0003$02.00

EARLY ENDOSPERM, EMBRYO, AND OVULE DEVELOPMENT IN GLYCINE MAX (L.) MERR.[1]

MARK A. CHAMBERLIN,* HARRY T. HORNER,[2,]* AND REID G. PALMER†

*Department of Botany and Bessey Microscopy Facility, and †Departments of Zoology and Genetics, and Agronomy, USDA-ARS, Iowa State University, Ames, Iowa 50011-1020

Anatomical and ultrastructural aspects of soybean embryo, endosperm, and ovule development are described for the zygote to late heart-shaped embryo stages (0–35 d postfertilization). Nucellar cells subtending the degenerative synergid break down, allowing for pollen tube passage to this synergid. In 15 of 17 ovules studied, the degenerative synergid occupies a position abfunicular to the zygote. The inner integument differentiates into the endothelium and exterior layers of thick-walled cells at the globular embryo stage. The endothelium has a cuticle on its inner surface that begins to fragment at the onset of endosperm cellularization. Cellularization of the free-nuclear endosperm is initiated at the globular embryo stage by the formation of anticlinal ingrowths of the central cell wall. These walls fuse to form cylinders open to the central cell. Uninucleate cells are formed within the bases of the cylinders as periclinal walls are laid down. These latter walls are formed in the presence or absence of phragmoplasts. At the onset of cellularization, the endosperm forms a cellular sheath over the apex of the embryo, which partitions it from the central cell. The late globular embryo forms a cuticle on its surface but not on the suspensor. The endosperm cells of the chalazal process are suspended in a mucilage because of the loss of the central cell wall in this region. Endosperm degeneration occurs by two different processes: one involves wall thinning coincident with accumulation of mucilage exterior to the plasmalemma and within the cytoplasm; the other involves the fusion of vesicles to the plasmalemma and the concomitant release of cell-wall fibrils. The embryo becomes reoriented 90° to accommodate its expansion within the embryo sac. The integrated development and function of these tissues toward embryo and ovule maturation are discussed.

Introduction

The growth and differentiation of the angiosperm ovule, embryo sac, and embryo occur in a series of interdependent stages and follow a characteristic pattern. In light of the fact that the embryo, endosperm, and ovule are three genetically distinct sets of tissue(s), their development and interaction must be highly orchestrated. This is exemplified in the soybean ovule, in which different tissues are successfully integrated in their actions to support the development of the embryo and bring about the formation of a viable seed. But few studies have related the interdependent formation and functional interaction of these tissues toward early embryo development in soybean.

Previous anatomical and ultrastructural studies of the soybean ovule have been concentrated on very early stages of development. The events of megasporogenesis and/or megagametogenesis (He et al. 1979; Kennell and Horner 1985; Folsom and Cass 1988, 1989), the prefertilization embryo sac (Folsom and Peterson 1984; Folsom and Cass 1990), and various aspects of fertilization in the egg apparatus (Dute et al. 1989) and central cell (Folsom and Cass 1992) have been documented. However, the body of literature on the postfertilization ovule of soybean is fragmented and only encompasses a short period of development following fertilization. The ultrastructure of the soybean embryo through the proembryo stage was studied by Folsom and Cass (1992) and Dute et al. (1989). Dute and Peterson (1992) characterized the development of the free-nuclear endosperm and the initial stages of its cellularization through the early globular embryo stage. Tilton et al. (1984) and Folsom and Cass (1986) discussed the formation and pattern of embryo sac wall ingrowths and their role in embryo nutrition.

Previous studies include little information on the development of embryo and endosperm beyond the early globular embryo stage. The intent of this study is to present information not included in these latter studies, although some overlap with them is necessary for descriptive continuity. Our study extends the body of knowledge on the developmental anatomy and ultrastructure of the soybean embryo, endosperm, and ovular tissues from the initiation of the zygote through the late heart-shaped embryo stage (35 d postfertilization). We also report on the interdependent pattern of development of these tissues and discuss their relationships in soybean ovule development.

Materials and methods

Glycine max (L.) Merr. cv Harosoy seeds were germinated and grown in a greenhouse or in the field. Floral buds or gynoecia, at various stages of development (0–35 d postfertilization), were

[1]Joint contribution of the Iowa Agriculture and Home Economic Experiment Station, Ames, Journal Paper no. J-15582, Project no. 2985, and the USDA-ARS FCR. The mention of a trademark or proprietary product does not constitute a guarantee or warranty of the product by the Iowa State University or the USDA and does not imply its approval to the exclusion of other products that may be suitable.

[2]Author for correspondence and reprints.

Manuscript received November 1993; revised manuscript received February 1994.

placed in 3% glutaraldehyde–4% paraformaldehyde in sodium cacodylate buffer (0.1 M, pH 7.2) at room temperature (RT; 22°C). The ovules were dissected in the fixative, placed under vacuum at 15 psi (6.89 kPa) for 1 h, and then placed in fresh fixative at 4°C for 12 h. Fixation was followed by three buffer rinses, postfixation in 1% osmium tetroxide in the same buffer for 4 h at RT, and dehydration in a graded ethanol series. En bloc staining (5% uranyl acetate in 70% ethanol) was done during the dehydration step in some material processed for electron microscopy. Acetone was used as a transitional solvent for infiltration into Spurr's resin (hard recipe). Infiltration in pure resin was accomplished on a rotator over a 2-wk period (fresh resin daily) before casting.

Light microscopy

Resin-embedded material was sectioned at 1 μm with glass knives on a Reichert Ultracut E microtome and fixed to poly L-lysine or gelatin-coated glass slides. A double stain of 0.13% methylene blue–0.02% azure II in 0.066 M NaH_2PO_4 buffer (pH 6.9), followed by 0.2% basic fuchsin in 2.5% ethanol, was used for its differential staining properties of thick sections embedded in Spurr's resin. All light microscope observations and photomicrography were made with a Leitz Orthoplan microscope fitted with bright-field, differential interference-contrast, and phase-contrast optics, and recorded on Kodak Technical Pan film.

Transmission electron microscopy (TEM)

Thin sections (60–90 nm) of resin-embedded material were cut with a Diatome diamond knife and stained with 5% uranyl acetate in 70% ethanol for 1 h and in aqueous lead citrate for 1 h. Sections were observed and photographed on a Hitachi HU-11C-1 TEM at 75 kV or a JEOL 1200EX-II STEM at 80 kV. Images were recorded on Kodak SO-163 film.

Scanning electron microscopy (SEM)

While in absolute ethanol, fixed and dehydrated ovules were placed in small ethanol-filled cylinders of Parafilm and sealed. The cylinders were immersed in liquid nitrogen for 5 min, then placed on a metal block in the liquid nitrogen, and fractured using a cold razor blade held by a hemostat. The fractured pieces of ovule were placed in absolute ethanol at 4°C and allowed to come to RT. The ovules were critical-point dried and mounted on brass disks with conductive tape and silver paint. Specimens were coated with gold or gold-palladium in a Polaron Sputter-coating Unit E5100 and observed with a JEOL JSM-35 SEM at 20 kV. Images were recorded on Polaroid 665 film.

Results

Zygote stage

The embryo sac is cone-shaped in sagittal section with the zygote and synergids positioned at its broad micropylar end. In longitudinal sections 90° to the sagittal plane, this sac is hourglass-shaped. Subtending the micropylar end of the embryo sac is a portion of the nucellus consisting of one or two cell layers. Some nucellar cells have degraded, forming a small gap opposite the degenerate synergid (fig. 1). This gap exposes this synergid to the outer integuments and micropyle. In sagittal sections of 17 ovules, where both the synergids could be identified, the degenerate synergid in 15 is abfunicular to the zygote and the persistent synergid is adfunicular. The cytoplasm of the degenerate synergid is condensed into electron-dense material. From the apex of the degenerate synergid, a trail of osmiophilic material extends to the apex of the zygote and to the primary endosperm nucleus (fig. 2). This trail has the same density as the cytoplasm of the degenerate synergid, indicating that it marks the path of the pollen tube nuclei.

Immediately after fertilization, the nucleoplasm of the primary endosperm nucleus is homogeneous and has no inclusions except for two nucleoli of different sizes (fig. 2). The smaller nucleolus is in a lobe of the primary endosperm nucleus. This lobed portion likely represents the fused sperm nucleus. The fusion is close to the cytoplasmic trail of the degenerate synergid (fig. 2). In subsequent stages, the primary endosperm nucleus is spherical and contains a single large nucleolus. Several divisions of the primary en-

→

Figs. 1–6 Soybean zygote (figs. 1–4) and proembryo (figs. 5, 6) stages. Fig. 1, Micropylar end of embryo sac with persistent (*p*) and degenerate (*d*) synergids. Note breakdown of nucellar cells (*n*) at arrow micropylar to degenerate synergid. *c* = central cell vacuole; *i* = inner integument; *o* = outer integument; bar = 10 μm. Fig. 2, Persistent (*p*) and degenerate (*d*) synergids subtending zygote (*z*). Note trail of dense material (arrows) leading from degenerate synergid to apex of zygote and primary endosperm nucleus (*es*). Asterisks denote aggregates of starch in central cell, and arrowheads denote nucleoli; bar = 10 μm. Fig. 3, Wandlabrinthe (*w*) displays different wall densities. *c* = central cell; bar = 1 μm. Fig. 4, After fertilization, amyloplasts (*) lose their starch, become smaller, and have no grana; mitochondria, ribosomes, and dilated ER are abundant; bar = 1 μm. Fig. 5, Micropylar end of central cell (*c*) showing proembryo and two adjacent free endosperm nuclei (arrow). Central cell vacuole is enlarged. *i* = inner integument; *o* = outer integument; bar = 20 μm. Fig. 6, Rosanoffian crystals and crystal cells in outer integumentary cells. Note crystal chambers fused to cell walls; bar = 10 μm.

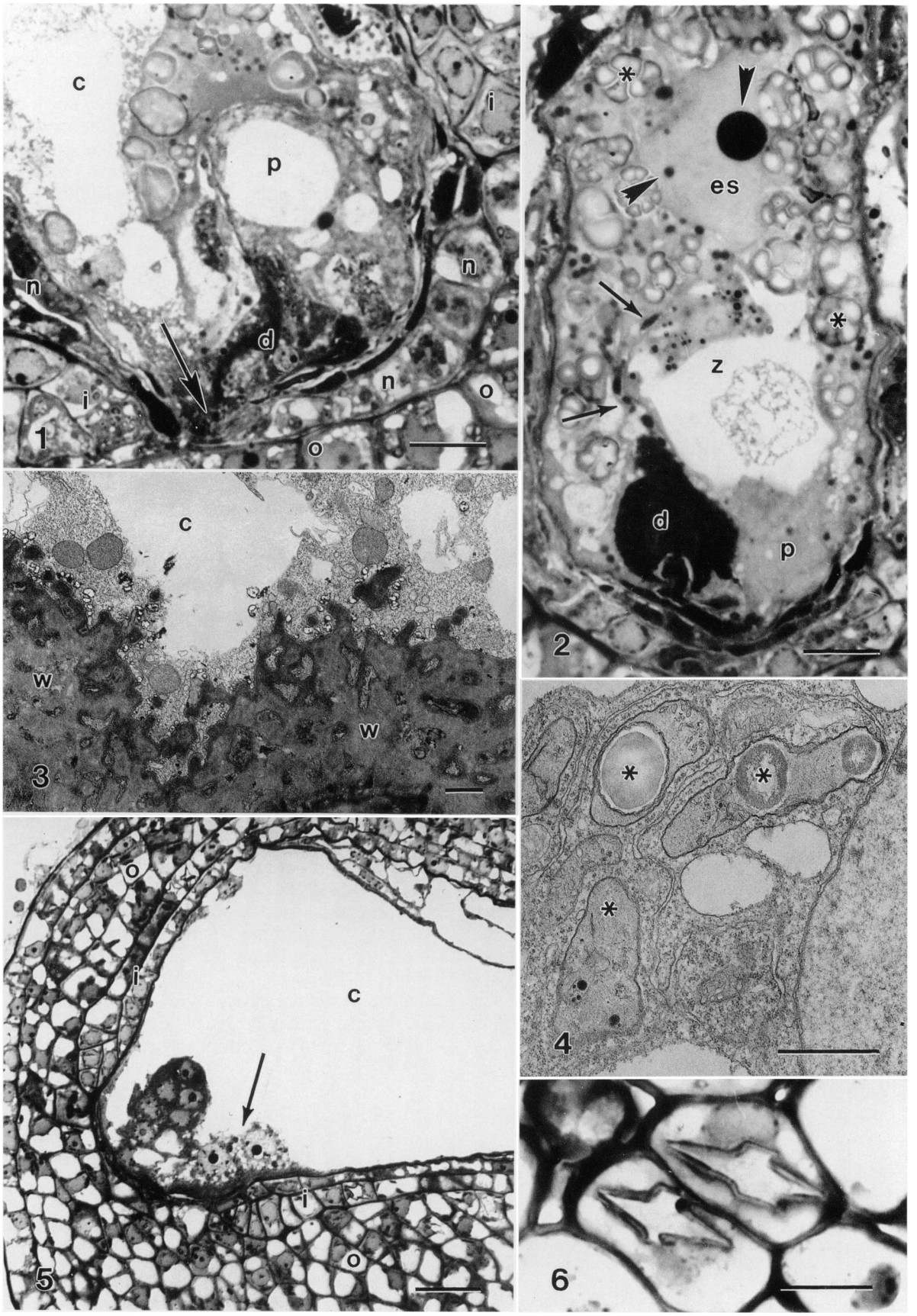

dosperm nucleus occur, thus initiating free-nuclear endosperm before the first zygotic division.

A digitate mass of wall ingrowths (wandlabrinthe) originates from the micropylar end of the central cell wall prior to fertilization and partially surrounds the basal-most portions of the synergids and zygote. It extends along the central cell wall to approximately half the height of the zygote. This digitate mass consists of regions of varying electron densities (fig. 3). The more electron-translucent parts are consistent in density with the central cell wall, whereas the denser regions are similar to the filiform apparatus at the base of the synergids. At later stages the wandlabrinthe is homogeneous in density.

The most conspicuous feature of the central cell at the zygote stage is the presence of numerous large amyloplasts (fig. 2). During endosperm development, the starch is depleted and the amyloplasts are smaller (fig. 4).

The inner integument is two to three layers thick and extends toward the micropyle from its point of origin along the hypostase to just short of the micropylar end of the embryo sac. The outer integument is five to 12 layers thick and similar to the inner integument in that its cells are moderately vacuolate.

Proembryo stage

At 2–3 d postfertilization, the zygote has divided to form a micropylar cell and an apical cell. Both cells undergo anticlinal divisions, followed by periclinal divisions, to form a short torpedo-shaped embryo (fig. 5). The resulting apical cells are densely cytoplasmic. The micropylar-most cells each contain a single large vacuole, and they develop transfer-cell-like wall ingrowths from their tangential and basal cross walls. These ingrowths become more extensive throughout development.

A large vacuole forms in the central cell before the first division of the zygote and continues to expand during the enlargement of the embryo sac and ovule. The vacuole expands and the free-nuclear endosperm is displaced to the periphery of the central cell (fig. 5). The abundant starch reserves present at the zygote stage are depleted as the vacuole enlarges. The starch reserves are absent from the central cell when the embryo is approximately 16-celled.

The nucellar cells demonstrate signs of degeneration prior to contact with the enlarging embryo sac. Their walls become thinner and an electron-dense mucilage-like material accumulates in the wall spaces. As the nucellus continues to degenerate, the embryo sac comes in contact with the inner integuments laterally and with the outer integuments at its micropylar end.

The number of cell layers of the outer integument increases as the ovule enlarges, primarily on the adfunicular side. Some of the cells of the inner layers of the outer integument form one to several, usually one, Rosanoffian crystal (Rosanoff 1865) per cell (fig. 6). The crystals are rectangular in one longitudinal plane and sharply diamond-shaped with two barblike protrusions radiating from their centers in the other longitudinal plane. As each crystal matures, it becomes bounded by a wall-like chamber within the cell. The chamber is usually fused to the inner surface of the cell wall. The outer layer(s) of the inner integument forms Rosanoffian crystals similar to those described in the outer integumentary cells. These crystals are found only in the interfacing cell layers of both integuments.

Globular embryo stage

At 8 d postfertilization, the embryo has differentiated into a globular embryo proper and short suspensor (fig. 7). The divisions at the apex of the embryo outpace those of the basal cells, giving the embryo its distinctive globular shape. Late in the globular embryo stage a thin cuticle forms over the surface of the embryo proper (fig. 8), but it is absent from the suspensor. The suspensor cells are larger and more vacuolate than the embryo-proper cells. In addition, the suspensor cells have an extensive array of transfer-cell-like wall ingrowths on the basal cross and tangential walls of individual cells.

The endosperm of soybean is of the free-nuclear type. It undergoes a number of synchronous free-nuclear divisions before cellularization (not shown). Cellularization is initiated at the micropylar end of the embryo sac and proceeds chalazally and centripetally (fig. 7). Early in the cellularization of the endosperm, a single wall is observed spanning the width of the central cell, covering closely the apex of the young globular embryo (fig. 9), thus separating the embryo region

→

Figs. 7–11 Globular embryo stage. Fig. 7, Embryo with young suspensor (*s*) surrounded by developing cellular endosperm (*es*). *c* = central cell vacuole; *i* = inner integument; *en* = endothelium; *o* = outer integument; *oi* = outer layer of inner integument; bar = 20 μm. Fig. 8, Cuticle (arrow) on surface of embryo proper (*e*). *es* = endosperm; bar = 1 μm. Fig. 9, Ensheathing endosperm (*es*) wall (arrow) covers apex of embryo (*e*); bar = 1 μm. Fig. 10, Peglike wall ingrowth of central cell wall with inflated tip during initial stages of endosperm (*es*) cellularization. Note vesicles within inflated tip (arrow). * = cuticle; *en* = endothelium; bar = 0.2 μm. Fig. 11, Inflated apex of growing endosperm (*es*) wall. Bulbous growth tip surrounded by central cell plasmalemma (arrow) and central cell vacuole (*c*) tonoplast (arrowhead); bar = 0.2 μm.

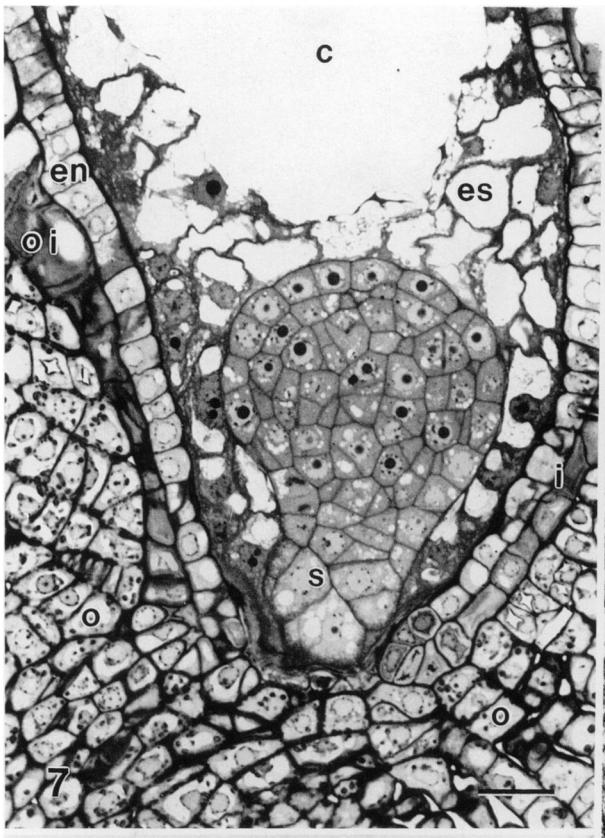

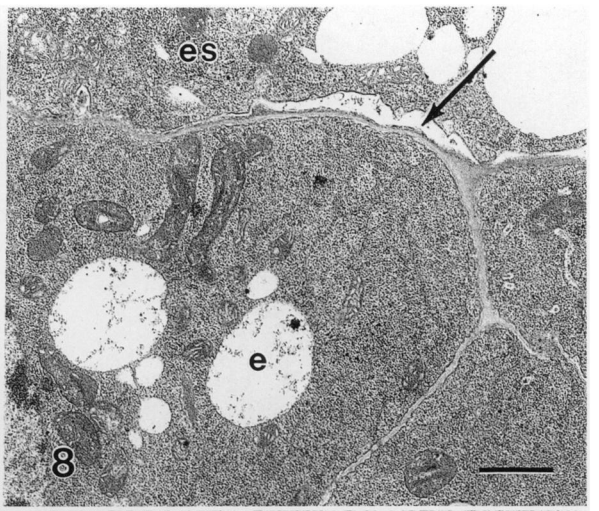

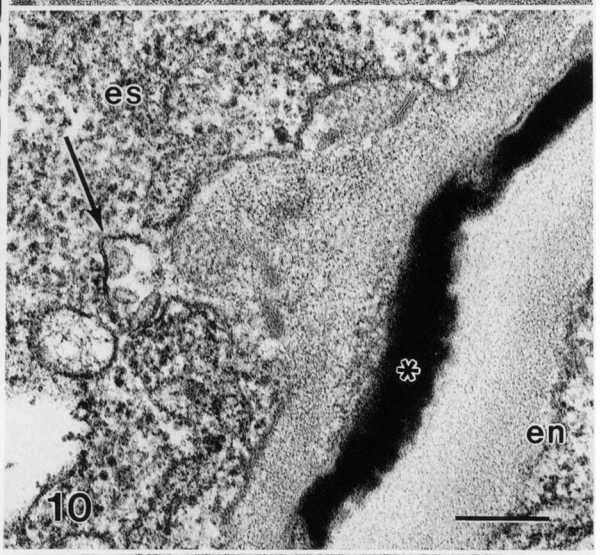

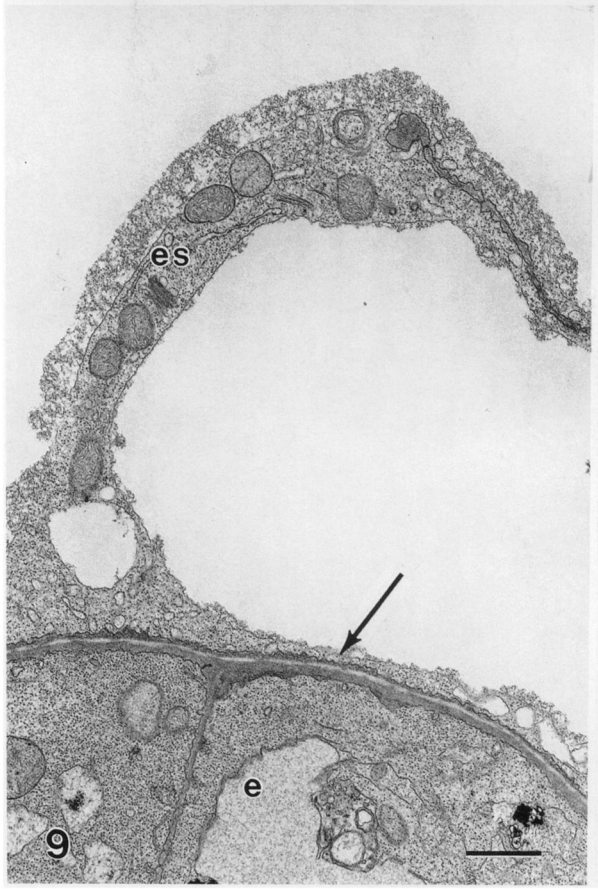

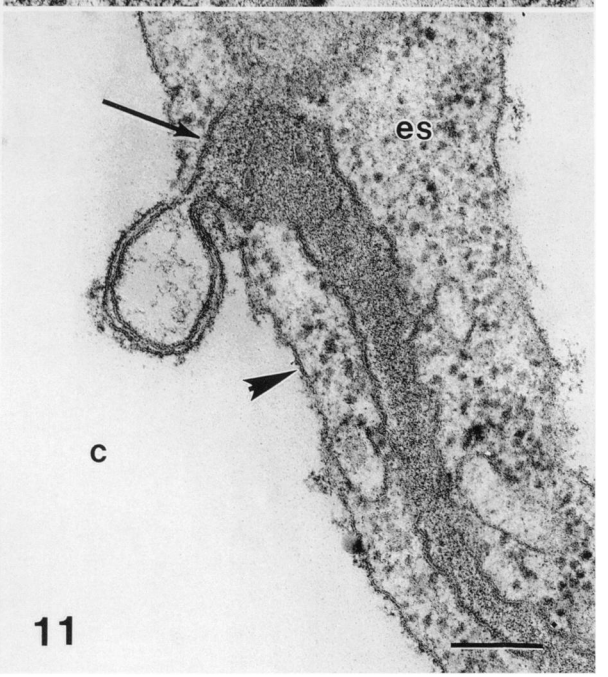

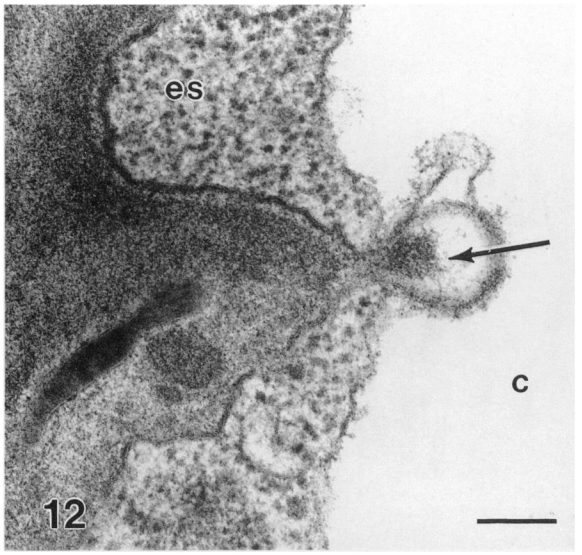

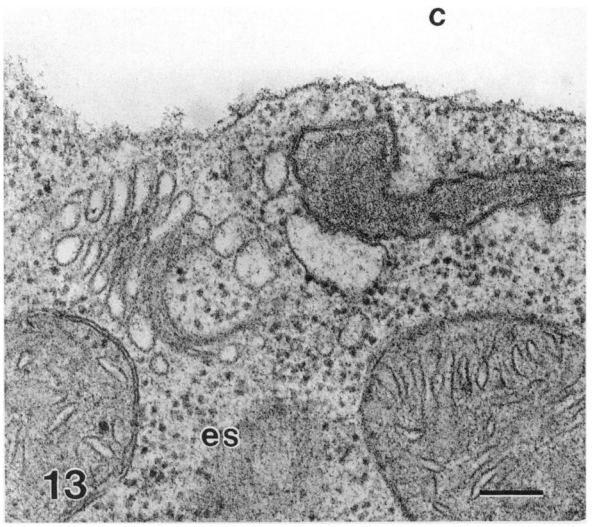

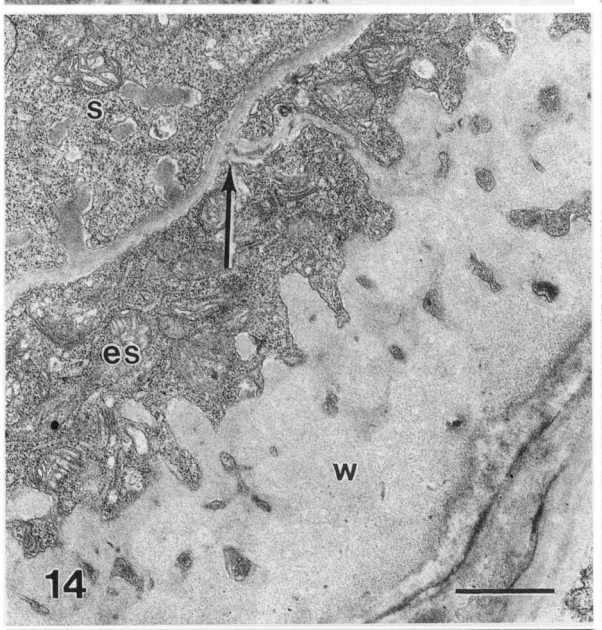

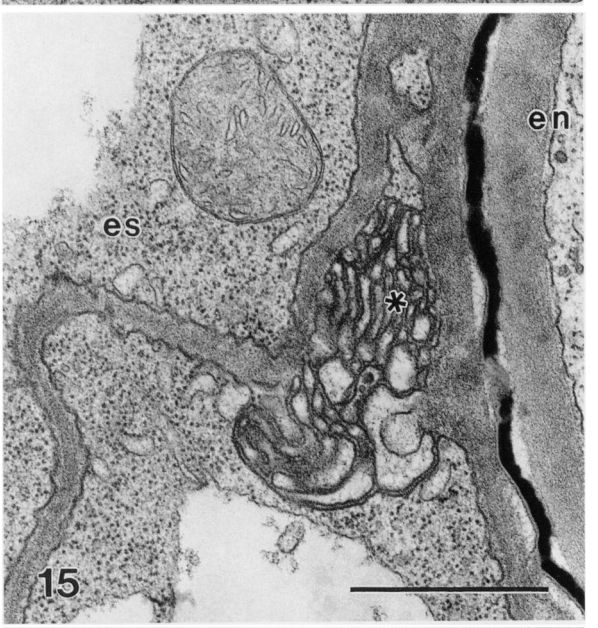

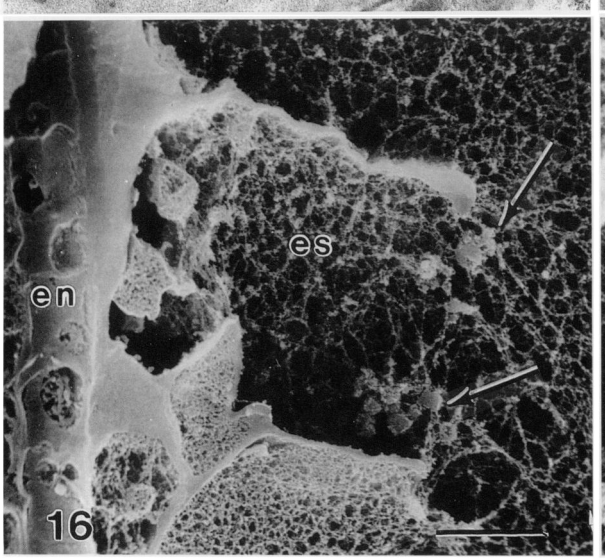

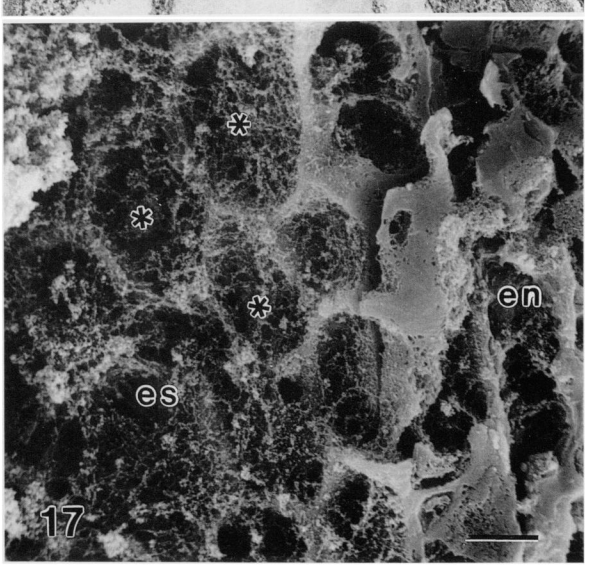

from the chalazal region of the embryo sac. This partitioning wall is unique because further cellularization across the width of the central cell does not occur until much later. Usually this partitioning wall is formed before the cuticle on the embryo proper. Eventually, walls will arise from the embryo-partitioning wall to connect with other endosperm walls (fig. 7).

Numerous vesicles are observed along the length of the central cell wall before endosperm cellularization. Peglike wall ingrowths from the central cell wall extend into the lumen of the central cell to form anticlinal walls (fig. 10). These ingrowths often are found opposite the gaps formed in the cuticle of the endothelium (Chamberlin et al. 1993*b*).

The growth of these walls seems to be a two-part process: first, the secretion of dense material from the wall itself, and second, the later fusion of dictyosome vesicles to the wall. Initially, the ends of these growing anticlinal walls form inflated tips (fig. 11) in which accumulate vesicles filled with material of the same density as the wall (fig. 10). The vesicles apparently rupture, and their contents are released within the inflated tips (fig. 12). Each inflated tip membrane is an extension of the central cell plasmalemma (fig. 11). The presence of dense material in these bulbous tips suggests that wall precursors are transported through the anticlinal wall and are continuously added to the growing tip. In addition, numerous dictyosomes and their vesicles are present along the lengths of the endosperm anticlinal walls (fig. 13). The lumens of these vesicles are less dense in comparison with the material found in the inflated tips. The dictyosome vesicles are observed fused to the plasmalemma near each tip and along the length of each growing wall.

Thin anticlinal walls are observed extending from the existing thicker wall ingrowths of the wandlabrinthe. These walls often are fused to the walls of basal cells of the suspensor (fig. 14). Only anticlinal walls originating from the wandlabrinthe are observed fused to the suspensor cells. No endosperm walls are observed fused to the embryo proper.

The surface area of the central cell plasmalemma increases greatly as the anticlinal walls grow into the central cell lumen. The vesicle membranes appear fused to the plasmalemma and are incorporated into it. Also, multilamellar bodies with stacks of membrane-like material are frequently observed at the junctures of the central cell wall and the newly formed anticlinal walls (fig. 15). These multilamellar bodies and vesicles may be a source of membrane material to accommodate the rapid increase in plasmalemma surface area of the central cell.

As the endosperm anticlinal walls extend into the central cell, they form sheetlike walls (fig. 16). The sheets fuse along their margins to form cylinders, which are open centripetally in the central cell lumen (fig. 17). Once these cylinders of wall material are laid down, completion of individual cells occurs by one of two methods. In the first method, the growing edge of each wall appears to branch at right angles to form periclinal walls (fig. 18). Later, these walls continue to grow and fuse with similar branches growing from the opposing cylinder walls, to each enclose a single nucleus, thus forming a cell. This process of wall growth and fusion follows a regular pattern. At no time are phragmoplasts or microtubules observed during this type of endosperm cellularization. In the second method of cellularization, the nucleus within a cylinder undergoes a mitotic division, during which a phragmoplast forms (fig. 19). This newly formed cross wall fuses with the anticlinal cylinder wall, resulting in the formation of a cell at the base of the cylinder and a free nucleus centripetally at the open end. Both methods of cell formation occur together, creating a single layer of endosperm cells at the periphery of the central cell. Once walled in by one of these methods, individual endosperm cells repeatedly undergo normal cytokinesis after mitosis. The two methods of cellularization and cytokinesis occur concurrently within the central cell (fig. 20) until the endosperm is completely cellular at the late heart-shaped embryo stage. Only uninucleate endosperm cells were observed.

An elongated channel is formed at the chalazal end of the embryo sac, which is bounded by the nucellus laterally and the hypostase chalazally (fig. 21). This channel contains large free nuclei (not shown) embedded in a degenerate cytoplasm that lacks organelles. Dense mucilage-like material is observed throughout the channel and seems to

←

Figs. 12–17 Globular embryo stage. Fig. 12, Anticlinal endosperm (*es*) wall ingrowth arising from central cell wall showing accumulation of electron-dense material (arrow) in bulbous tip. *c* = central cell vacuole; bar = 0.2 μm. Fig. 13, Freely growing endosperm wall closely associated with dictyosome and vesicles. *c* = central cell vacuole; *es* = endosperm; bar = 0.2 μm. Fig. 14, Wandlabrinthe (*w*) with endosperm (*es*) wall ingrowth fused to base of suspensor (*s*) cell wall (arrow); bar = 1 μm. Fig. 15, Multilamellar body (*) in axil of anticlinal endosperm (*es*) wall ingrowth. Note gap in cuticle at surface of endothelium (*en*); bar = 1 μm. Fig. 16, Sheetlike anticlinal endosperm (*es*) wall ingrowths protruding into central cell. Note vesicles near tips of developing walls (arrows). *en* = endothelium; bar = 10 μm. Fig. 17, Inner surface view of central cell showing cylinder-like ingrowths (*) of early cellularization of endosperm (*es*). *en* = endothelium; bar = 10 μm.

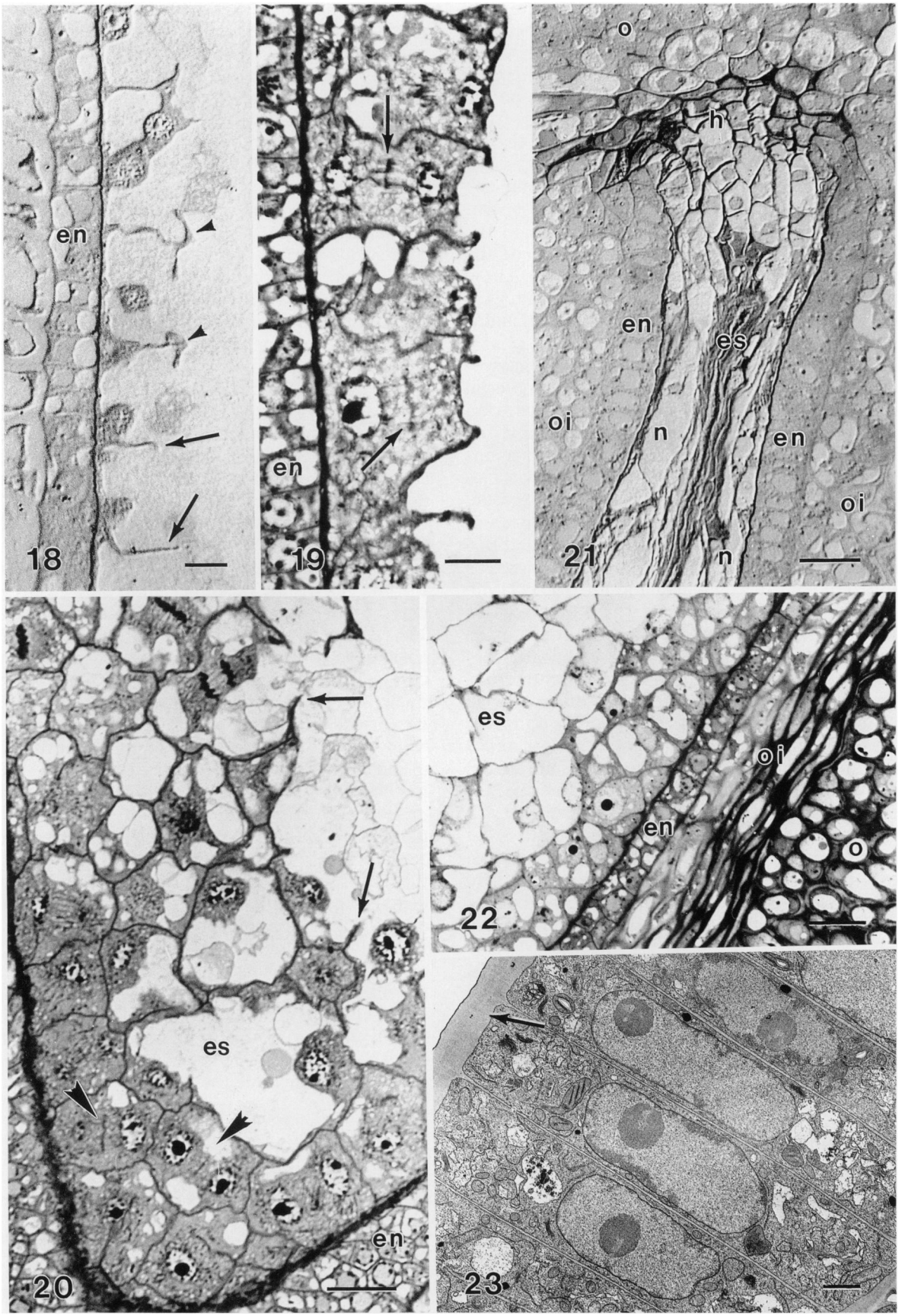

accumulate during the degradation of the surrounding nucellar tissue. The chalazal channel and the hypostase have been collectively called the endosperm haustorium (Dute and Peterson 1992). This "haustorium" does not invade the ovular tissues, and, therefore, we prefer to use the neutral term "chalazal process." Although not invading the surrounding tissues, outer integument cells in contact with the chalazal-most end of the hypostase become necrotic and eventually collapse (fig. 21).

The inner integument differentiates into two distinct tissues (figs. 7, 18). The outer tissue is composed of one to seven layers of thick-walled cells. Each cell has a single, large vacuole and a reduced complement of organelles. The single inner cell layer (endothelium) that abuts the embryo sac or nucellus consists of less vacuolate cells with a greater number of organelles than the cells of the outer layer. The inner surface of the endothelium has cuticle, which begins to fragment (fig. 15).

Early heart-shaped embryo stage

The cotyledonary primordia appear 12–15 d postfertilization, giving the embryo its distinctive heart shape. The two young cotyledons lie in the sagittal plane of the ovule at this stage of development.

The endosperm is completely cellular except for the chalazal process, which remains free-nuclear. Endosperm cells in the middle of the central cell are large and thin-walled, and each has a single, large vacuole (fig. 22). These endosperm cells rarely divide after they become cellular, whereas the peripheral layers of cells remain meristematic and proliferate to keep pace with the expansion of the embryo sac and ovule. Plasmodesmata are more common between the peripheral cells than between those more centrally located. The entire cellular endosperm does not seem to accumulate storage products at this stage or at later stages.

The outer integument is composed of three tissue regions. The epidermis has differentiated into the palisade layer, which is two cell layers thick in the hilar region. The outer layer in the hilar region is contributed by the funiculus. The columnar cells of the palisade layer have lignified periclinal walls, much thicker than their anticlinal walls (fig. 23). Each cell is rich in organelles and has a large oblong nucleus. The central region of the outer integument consists of numerous layers of highly vacuolate isodiametric cells below the palisade epidermis and away from the hilar region. Within these layers the vasculature of the ovule differentiates. The innermost region of the outer integument consists of six to nine layers of isodiametric cells with numerous intercellular spaces. These cells are smaller and cytoplasmically denser than the adjacent cells of the outer integument. Dark-staining mucilage-like material fills the intercellular spaces of this region (fig. 22).

At the micropylar end, the thick-walled cells of the inner integument develop into elongated cells (fig. 22) that divide no further. These cells appear stretched, probably to accommodate the elongation of the ovule. Chalazally, these cells retain their earlier morphology but the number of layers has increased. The endothelium remains unchanged.

Late heart-shaped embryo stage

The embryo has a distinct dome-shaped shoot apical meristem (fig. 24) by 20 d postfertilization, and the radicle meristem is formed shortly thereafter. The embryo with partially enlarged cotyledons fills the micropylar half of the embryo sac. The hypocotyl is well developed. The cotyledons expand laterally. As the embryo grows, it becomes reoriented (fig. 25) 90° so that the surfaces of the cotyledons are now parallel to the broad sides of the ovule. This is the position that the cotyledons will have in the mature seed.

The suspensor cells elongate (fig. 24). Only the basal tier of cells have transfer-cell-like wall ingrowths that are especially prominent on the tangential walls in contact with the endosperm and on the basal cross walls. The late heart-shaped embryo has a thin cuticle, but unlike earlier stages it covers the suspensor also, except for the basal tier of cells.

The integuments begin to take on the characteristic morphology of the mature testa. The testa is composed of five layers beginning with the pal-

←

Figs. 18–23 Globular (figs. 18–21) and early heart-shaped embryo (figs. 22, 23) stages. Fig. 18, Anticlinal endosperm wall ingrowths (arrows) and subsequent periclinal branching of these walls (arrowheads). *en* = endothelium; bar = 10 μm. Fig. 19, Phragmoplast formation (arrows) between dividing endosperm nuclei. *en* = endothelium; bar = 10 μm. Fig. 20, Endosperm (*es*) cellularization showing freely growing walls (arrows) and phragmoplast formation (arrowheads) after septation has occurred. *en* = endothelium; bar = 20 μm. Fig. 21, Chalazal process with free-nuclear endosperm (*es*) bordered by nucellar (*n*) cells laterally and hypostase (*h*) chalazally. *en* = endothelium; *oi* = outer layers of inner integument; *o* = outer integument; bar = 20 μm. Fig. 22, Cross section of ovular tissues showing cellular endosperm (*es*), different layers of inner integument, and innermost layer of outer integument (*o*) infiltrated with dense mucilage around cells; *en* = endothelium; *oi* = outer layers of inner integument; bar = 20 μm. Fig. 23, Palisade epidermis with thick outer periclinal wall (arrow) showing cuticle; bar = 2 μm.

Figs. 24–27 Late heart-shaped embryo stage. Fig. 24, Embryo with dome-shaped apical shoot meristem (arrowhead) and procambial initials in hypocotyl (*). *es* = cellular endosperm; *o* = outer integument; *s* = suspensor; bar = 100 μm. Fig. 25, Longitudinal section 90° to sagittal plane through ovule showing partially rotated embryo cotyledons (*) and cellular endosperm (*es*). Note constriction of embryo sac. *o* = outer integument; bar = 100 μm. Fig. 26, Cross section of testa showing palisade epidermis (*pa*), hypodermis (*hy*), parenchymatous layer (*), and adjacent inner integument layer (far right); bar = 20 μm. Fig. 27, Tracheary bar (*) with pore opening to hilum (arrow). Note two-layered palisade epidermis (*pa*) in hilar region; bar = 100 μm.

isade epidermis (fig. 26). The palisade layer fills with electron-dense spherical bodies (not shown), similar to those formed in the outer integumentary cells opposite the micropylar end of the embryo sac (Chamberlin et al. 1993*b*). The hypodermis is composed of a single layer of osteosclereids, or "hourglass" cells, with lignified anticlinal walls. Next is a spongy tissue composed of several layers of lacunate parenchyma with large tangentially elongated lobes (fig. 27). The vasculature of the ovule and the tracheary bar (fig. 27) are within this layer of tissue. This bar

extends from near the micropyle to midway up the length of the ovule below the hilar groove. The tracheid bar is ovate in ovule cross section with its narrow apex exposed to the surface of the hilum. The bar is composed of numerous enlarged tracheoids with reticulate wall thickenings (fig. 27). The outer layers of the inner integument are crushed during the expansion of the ovule, and only a remnant of these thick-walled cells remain (fig. 25). The endothelium remains unchanged, but it too is eventually crushed during ovular growth.

The endosperm breaks down as the embryo expands, and a symmetrical void forms around the apex of the embryo. No physically ruptured endosperm cells were observed near the embryo. The endosperm breaks down by two morphologically distinct processes that cause the progressive thinning of the endosperm walls. The first process involves progressive wall degradation associated with dictyosome vesicle activity (Chamberlin et al. 1993*b*). The second process of endosperm degradation occurs predominantly in endosperm cells of the chalazal half of the embryo sac. The latter process is similar to that observed in the nucellar cells and involves the formation of electron-dense, mucilage-like material in the space between the wall and plasmalemma (fig. 28). This material appears to be deposited by dilated RER fused to the plasmalemma. Coincident with mucilage accumulation in the wall space, the cell wall deteriorates. Mucilage-filled vesicles are formed by invaginations of the plasmalemma, and they accumulate in the cytoplasm. The vesicles eventually rupture, and the mucilage diffuses into the cytoplasm (fig. 28) until the cell wall is completely degraded and the cytoplasm becomes osmiophilic.

The chalazal process has elongated with the expansion of the ovule and has become cellular. In light micrographs, this process has thin-walled cells that stain intensely owing to the presence of electron-dense material between their walls and plasmalemmas (not shown). The extreme chalazal end of this process has a sparse number of endosperm cells embedded in a dense granular matrix (fig. 29). These endosperm cells are not attached to the central cell but are suspended in this matrix because of the disappearance of the central cell wall during the rapid elongation of the ovule (fig. 30). The cuticle at the inner surface of the endothelium persists in the region of the chalazal process.

Discussion

Because the ovule of soybean is crassinucellate, the pollen tube must penetrate intervening layers of nucellus between the micropyle and the embryo sac. Nucellar cells degenerate micropylar to the abfunicular synergid, providing a path for the passage of the pollen tube into the embryo sac. Before fertilization in cotton, a similar group of nucellar cells degenerates to accommodate the passage of the pollen tube (Jensen 1969). The dissolution of these cells in soybean may be promoted by secretions of the synergid that degenerates just before fertilization (Tilton 1981; Dute et al. 1989). The synergids have been suggested to be secretory cells involved in pollen tube attraction in a number of diverse taxa (Tilton 1981).

The first degenerating synergid consistently receives the pollen tube and its contents, as noted in numerous taxa (Mogensen 1984). Jensen (1974) suggested that a degenerate synergid is a requisite condition for pollen tube penetration. In 15 of 17 ovules observed in our study, the abfunicular synergid degenerated first. The preference for degeneration of one synergid over the other has not been shown in other soybean genotypes (Dute et al. 1989; Folsom and Cass 1992) but has been observed in *Hordeum vulgare* (Mogensen 1984), *Linum usitatissimum* (Russell and Mao 1990), and *Helianthus annuus* (Yan et al. 1991). What determines which synergid is to degenerate first is unclear. Morphological data on the two synergids do not give a clue. The synergids of soybean (Folsom and Cass 1990), *Solanum* (Briggs 1992), *Brassica* (Sumner and Van Caeseele 1989), and other taxa (Tilton 1981) seem to be cytologically equal. Since this is integral to understanding fertilization in angiosperms, physiological and histochemical studies, along with quantitative studies, are warranted to understand the nature of the selective degeneration.

The wandlabrinthe is a conspicuous ingrowth of the micropylar central cell wall, surrounding the base of the zygote and synergids. This labyrinth of wall ingrowths is a common feature in a number of diverse taxa. It is common in the legumes *Pisum* (Marinos 1970), *Vicia, Phaseolus, Spartium,* and *Lathyrus* (Gunning and Pate 1974). Following fertilization, the wandlabrinthe of soybean becomes more massive. This is probably due to the deposition of densely staining material from the filiform apparatus as the synergids degenerate. In soybean, the wandlabrinthe may facilitate the transport of solutes into the embryo sac from the integuments near the micropyle (Tilton et al. 1984; Chamberlin et al. 1993*b*). During cellularization of the endosperm, we noted anticlinal walls from the wandlabrinthe fused to the base of the suspensor. These may act as direct apoplastic channels of nutrient transport.

More than simply housing the zygote, the central cell is dynamic in its postfertilization development. This is indicated by its organellar complement, transfer-cell-like wall ingrowths, rapid divisions of the free-nuclear endosperm, and breakdown of its starch reserves. According to

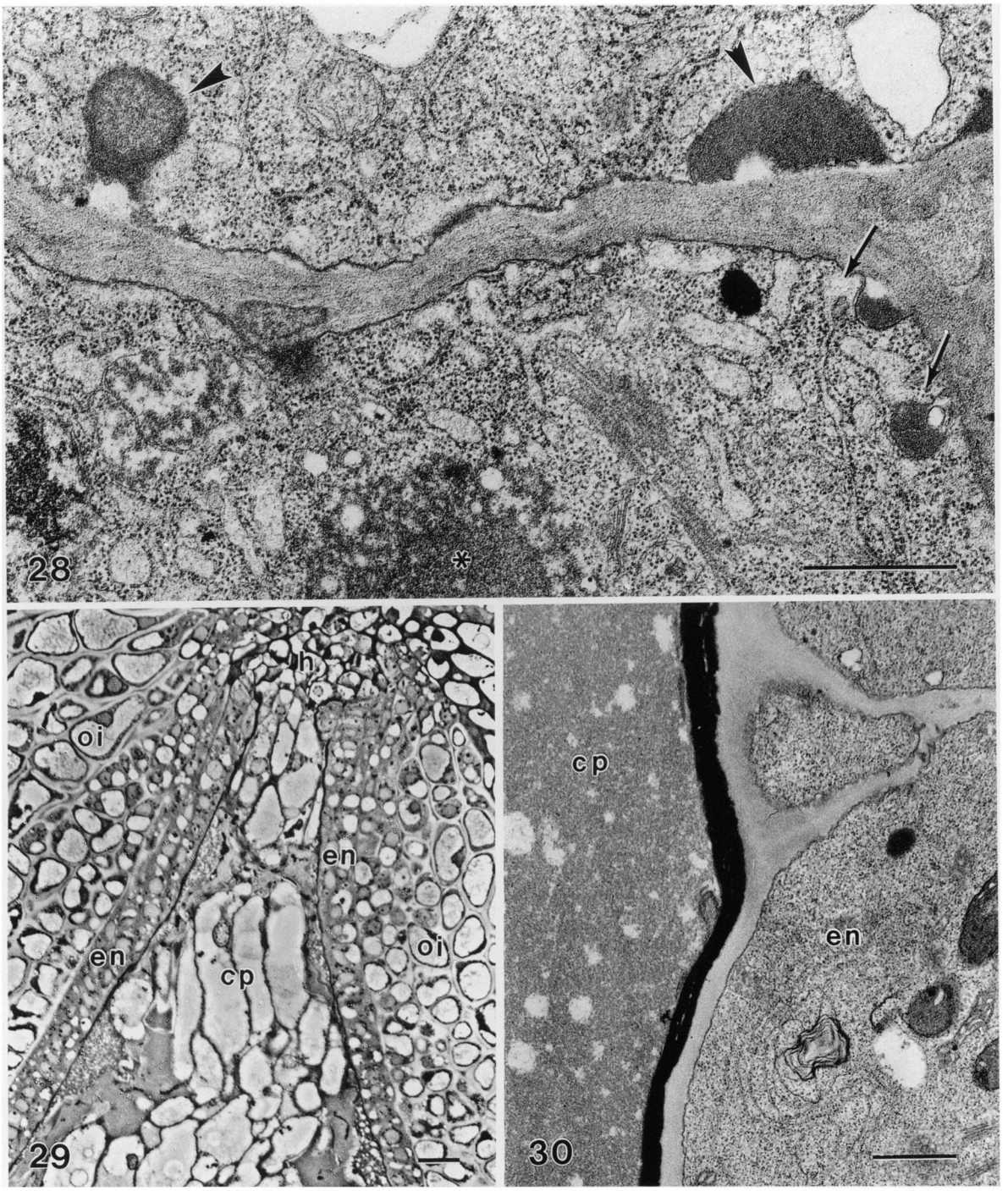

Figs. 28–30 Late heart-shaped embryo stage. Fig. 28, Electron-dense material accumulated between plasmalemma and wall of endosperm cells in association with dilated RER (arrows). Plasmalemma invaginations (arrowheads) show regions where dense material will be released into cytoplasm, where it diffuses (*); bar = 1 μm. Fig. 29, Chalazal process (*cp*) with endosperm cells embedded in a dense matrix. *h* = hypostase; *en* = endothelium; *oi* = outer layers of inner integument; bar = 20 μm. Fig. 30, Granular matrix in chalazal process (*cp*). Note absence of central cell wall and persistence of endothelium (*en*) cuticle lining chalazal process; bar = 1 μm.

Folsom and Cass (1992), vacuoles fuse with the multigrain amyloplasts and aid in their breakdown. This pattern has been noted in the endosperm of a number of taxa. Subsequently, the vacuoles coalesce into the large central vacuole that occupies the space left by the amyloplasts (Folsom and Cass 1992). The hydrolysis of the starch reserves likely forms a pool of water-sol-

uble carbohydrates in the central cell that could be readily absorbed by the free-nuclear endosperm. This rich carbon source also is accessible to the young embryo as indicated by plasmodesmatal connections between the central cell and the zygote, proembryo (Dute et al. 1989), and the early globular embryo (Chamberlin et al. 1993*b*).

Divisions of the soybean free-nuclear endosperm precede those of the zygote and are rapid and synchronous. This synchrony of free-nuclear endosperm divisions has been observed in wheat as well (Bennett et al. 1973). Gunning and Steer (1975) noted that nuclei sharing a common mass of cytoplasm often have synchronous divisions. Chamberlin et al. (1993*a*) observed that the soybean endosperm nuclei were evenly spaced throughout the central cell, except for their sparse occurrence in the chalazal process. The rapid synchronous divisions and the nonrandom position of the nuclei imply a regulatory mechanism is involved in the positioning of the endosperm nuclei. An immunocytochemical study in wheat has shown that the endosperm free nuclei are interconnected by a cytoskeleton of tubulin (Van Lammeren 1988). Microtubules were shown to radiate from the nuclei that apparently anchor them in stage- and locus-specific positions in the central cell. The interconnection of the endosperm nuclei indicates that a communication among them is responsible for their synchronous divisions and short-distance movement.

Cellularization of the soybean endosperm is initiated by the formation of anticlinal wall ingrowths from the central cell wall. The tip of each of these walls grows in the absence of microtubules, similar to the growth seen in *Stellaria* (Newcomb and Fowke 1973) and *Haemanthus* (Newcomb 1978). But this is in contrast to reports of apical wall growth in the endosperm in the presence of microtubules in other soybean genotypes (Dute and Peterson 1992), wheat (Mares et al. 1977), cotton (Jensen et al. 1977), and *Arabidopsis* (Mansfield and Briarty 1990). We do not believe that our different results, when compared with other soybean genotypes, are a genotype-specific trait or that they resulted from poor tissue preparation, because microtubules were noted at other stages of endosperm development and in other tissues. A possible explanation is that apical growth of these walls is not a continuous process and that during periods of cessation of growth the microtubules are absent. After a period of growth, the anticlinal walls grow laterally to form sheetlike walls that fuse at their edges to form cylinders open to the central cell centrally. These walls branch and fuse to enclose a single nucleus within each new cell. This pattern of cross-wall formation and fusion is observed in *Stellaria* (Newcomb and Fowke 1973) and in the first four peripheral layers of endosperm in *Haemanthus* (Newcomb 1978).

In this study, the formation of the peripheral layer of endosperm also utilizes a second type of periclinal wall formation within the cylinders: the formation of a phragmoplast between sister nuclei after karyokinesis. This pattern is the sole method by which these cross walls are formed in *Helianthus* (Newcomb 1973), wheat (Mares et al. 1977; Fineran et al. 1982; Van Lammeren 1988), and in soybean as reported by Dute and Peterson (1992). In soybean, once a nucleus has been compartmentalized by one of the two latter processes, it undergoes a normal mitotic division with the formation of a phragmoplast. Although various patterns of wall formation exist among different taxa, and even within a single embryo sac (this study; Newcomb 1978), normal mitotic divisions after compartmentalization seem to be the only consistent pattern among the previously mentioned studies.

Three distinct patterns of endosperm wall formation were noted in this study: (1) wall ingrowths of the central cell wall that grow and branch in the absence of microtubules, (2) phragmoplast-aided formation of cross walls between sister nuclei within preformed cylinders, and (3) normal mitosis within already compartmentalized cells. It is curious that all three types of wall formation can occur at the same time within a given central cell and give rise to uninucleate endosperm cells. This would indicate a highly coordinated regulatory system in a seemingly chaotic coenocytic central cell. In wheat, the free nuclei of the endosperm are interconnected by cytoskeletal elements (Van Lammeren 1988). A similar association of elements may exist in the endosperm of soybean. These connecting elements may aid in coordinating the biosynthetic machinery of the numerous nuclei and, therefore, orchestrate the cellularization of the endosperm.

In this study, anticlinal wall ingrowths of the central cell wall lack a phragmoplast-like mechanism at their growing tips, as seen in wheat (Mares et al. 1977). Immunocytochemical studies of plant cell wall biosynthesis have shown that wall matrix polysaccharides, such as pectins and hemicelluloses, are formed at the dictyosomes, but priming reactions probably occur at the ER (Brett and Waldron 1990). In the soybean endosperm, these organelles are in close association with the growing tips of the wall. It is possible that dictyosome vesicles transport these matrix polysaccharides to the wall where they fuse with the plasmalemma and are integrated with cellulose in the wall. Available evidence indicates that cellulose is formed at or just outside the plasmalemma (Brett and Waldron 1990). Gaps in the endothelial cuticle of soybean frequently are observed opposite the base of these growing walls

(Chamberlin et al. 1993*b*). These interruptions in the cuticle allow the direct absorption of nutrients from the integumentary tissues via these wall ingrowths in *Capsella* (Schulz and Jensen 1974). It is possible that carbohydrates are transported from the soybean endothelium, travel apoplastically within the endosperm anticlinal walls, and are then deposited at the plasmalemmas of the growing walls. The carbohydrates are likely converted into cellulose, which is deposited in the plasmalemma swelling at the tip of the growing wall. The cellulose then is linked with the matrix polysaccharides during apical wall growth.

Cellularization of the endosperm proceeds rapidly in the micropylar region of the embryo sac, but the chalazal channel remains acellular until the late heart-shaped embryo stage. The hypertrophied nuclei and the lack of organelles indicate that this channel is physiologically distinct. Autoradiographic evidence indicates that labeled assimilates from the chalazal vascular strand enter the channel via the hypostase and move unimpeded through the common cytoplasm of the channel to the main portion of the embryo sac (Chamberlin et al. 1993*b*). Indeed, numerous studies have suggested that the free-nuclear condition of the chalazal process is essential to its function in the translocation of nutrients to the embryo sac (Vijayaraghavan and Prabhakar 1984). Endosperm cellularization in the chalazal channel of soybean likely precludes its function in nutrient transport, as evidenced by the nutritionally deprived necrotic condition of these cells.

The cellular endosperm of soybean has no evident storage products and seems to have no direct role in embryo nutrition. But the endosperm does appear to translocate nutrients into the embryo sac by the common apoplast of its cell walls as suggested by autoradiographic evidence (Chamberlin et al. 1993*b*). Nutrients from the integuments are likely channeled through the transfer-cell-like wall ingrowths of the lateral central cell wall and the wandlabrinthe. The endosperm as a mechanism for nutrient absorption by the embryo sac has been suggested in *Pisum* (Marinos 1970), *Quercus* (Singh and Mogensen 1976), and *Zea* (Schel et al. 1984).

As the endosperm degenerates, it leaves a void around the apex of the embryo proper, which indicates that the embryo secretes enzymes responsible for the endosperm digestion. The presence of a cuticle on the embryo proper and the lack of secretory activity (reduced vesicle content) within its cells indicate that the embryo is not the enzymatic source for endosperm digestion in this region. Indeed, the endosperm cells near the apex of the embryo seem to be autolytic and to digest from the inside out. A similar pattern of autolysis was noted in lettuce endosperm (Jones 1974). The presence of dense mucilage-like material in the wall space along the plasmalemma and the coincident thinning of the endosperm walls seem to justify the latter conclusion. The coincident accumulation of osmiophilic material in the wall space and the degeneration of the endosperm also have been observed in *Zea* (Schel et al. 1984) and *Euphorbia* (Gori 1987).

The endosperm cells near the suspensor degenerate differently from more chalazal endosperm cells in the embryo sac. The embryo cuticle is absent from the basal cells of the suspensor, suggesting that these cells are directly involved in endosperm digestion. But, like cells of the embryo proper, basal suspensor cells lack the cytology indicative of a secretory function. In the endosperm cells, the presence of numerous dictyosome vesicles fused to the plasmalemma and the concomitant release of fibrillar material from the exterior of the wall indicate an autolytic process (Chamberlin et al. 1993*b*). We believe these are cell wall polysaccharides released by hydrolytic enzymes synthesized in the endosperm cells. Outside the cell, the fibrils condense and are transformed into a mucilage-like material.

During cellularization of the endosperm, the early globular embryo is partitioned from the rest of the central cell by the formation of an ensheathing endosperm wall and eventual cellular endosperm. Similar endospermic sheaths surrounding the embryo have been observed in *Phaseolus* (Yeung and Clutter 1978) and *Pisum* (Marinos 1970). The authors of those studies suggested that the sheath regulates the flow of nutrients from the liquid endosperm to the embryo. Marinos (1970) further suggested that the sheath serves to maintain the orientation of the embryo.

The globular embryo generally forms a cuticle after the formation of the ensheathing cellular endosperm. But the cuticle is absent from the suspensor; this, along with the pattern of wall ingrowths in the suspensor, indicates that the suspensor absorbs nutrients from the micropylar base of the embryo sac and transports them acropetally to the embryo proper. This is supported by autoradiographic evidence (Chamberlin et al. 1993*b*). The cellular endosperm surrounding the embryo proper seems to lack nutrients. Therefore, cuticularization of the embryo proper may be a consequence of the partitioning of the embryo from the central cell, thus limiting the outflow of nutrients from the embryo proper to the nutrient-poor cellular endosperm. At the late heart-shaped embryo stage, the cuticle covers the surface of the embryo except for the basal-most tier of suspensor cells. The suspensor remains as the primary route of nutrient flux to the embryo (Chamberlin et al. 1993*b*). The presence of an embryo cuticle indicates that the embryo is becoming more autonomous in its development to-

ward maturation. The formation of the ensheathing endosperm and cuticle on the embryo likely precludes access of the embryo to nutrients in the chalazal region of the embryo sac and mandates that the embryo receive its nutrients from the micropylar end of the embryo sac.

The embryo sac is constricted midway up its length, giving it an hourglass shape. At the early heart-shaped embryo stage the cotyledons are initiated. Because of expansion of the cotyledons, the embryo becomes oriented 90° to accommodate the passage of the cotyledons through the central constriction in the embryo sac. This orientation also allows the cotyledons to fit better into the chalazal end of the embryo sac, which is broader in the longitudinal plane 90° to the sagittal plane.

Differentiation of the integuments first occurs in the inner integument with the formation of the endothelium and layers of thick-walled cells at the early globular embryo stage. The formation of the endothelial layer at an early stage of ovular development and its persistence through the late heart-shaped embryo stage indicate that this layer has a role in the development of the adjacent embryo sac. The abundance of organelles in a dense cytoplasm also indicates a functional tissue, probably involved in the transport of nutrients to the embryo sac. A similar function has been attributed to the endothelial layer in *Bellis perennis* (Engell and Petersen 1977) and *Saintpaulia ionantha* (Mogensen 1981). The thick-walled cells of the inner integument probably play a supportive role in embryo sac nutrition by protecting the endothelium from being crushed by the differentially expanding outer integuments.

The endothelial cuticle probably prevents solute movement into the embryo sac at the early stages of ovule development. The degeneration of this cuticle occurs during the cellularization of the endosperm and rapid growth of the embryo, when the embryo sac is probably a significant nutrient sink. Autoradiographic evidence indicates that nutrients pass into the embryo sac at the onset of degeneration of this barrier (Chamberlin et al. 1993*b*). The initial vascularization of the outer integument coincides with the breakdown of the endothelial cuticle. Since there are no vascular connections with the inner integuments, nutrients from the vasculature probably diffuse along a concentration gradient toward the endothelium before entering the lateral regions of the embryo sac (Thorne 1981).

Acknowledgments

We thank Bruce Wagner for his assistance in the use of the electron microscopes. A special thanks to Dr. Nels Lersten for his wealth of knowledge and feedback in preparing this manuscript. The microscopy was carried out in the Bessey Microscopy Facility, a Biotechnology and Life Sciences Center at Iowa State University.

Literature cited

Bennett MD, MK Rao, JB Smith, MW Bayliss 1973 Cell development in the anther, the ovule, and the young seed of *Triticum aestivum* L. var. Chinese spring. Philos Trans R Soc Lond Ser B Biol Sci 266:39–81.

Brett C, K Waldron 1990 Physiology and biochemistry of plant cell walls. Unwin Hyman, London. 194 pp.

Briggs CL 1992 A light and electron microscope study of the mature central cell and egg apparatus of *Solanum nigrum* L. (Solanaceae). Int J Plant Sci 153:40–48.

Chamberlin MA, HT Horner, RG Palmer 1993*a* Nuclear size and DNA content of the embryo and endosperm during their initial stages of development in *Glycine max* (Fabaceae). Am J Bot 80:1209–1215.

——— 1993*b* Nutrition of ovule, embryo sac, and young embryo in soybean: an anatomical and autoradiographic study. Can J Bot 71:1153–1168.

Dute RR, CM Peterson 1992 Early endosperm development in ovules of soybean, *Glycine max* (L.) Merr. (Fabaceae). Ann Bot 69:263–271.

Dute RR, CM Peterson, AE Rushing 1989 Ultrastructural changes of the egg apparatus associated with fertilization and proembryo development of soybean, *Glycine max* (Fabaceae). Ann Bot 64:123–135.

Engell K, GB Petersen 1977 Integumentary and endotheliar cells of *Bellis perennis:* morphology and histochemistry in relation to the developing embryo sac. Bot Tidsskr 71:237–244.

Fineran BA, DJC Wild, M Ingerfeld 1982 Initial wall formation in the endosperm of wheat, *Triticum aestivum:* a reevaluation. Can J Bot 60:1776–1795.

Folsom MW, DD Cass 1986 Changes in transfer cell distribution in the ovule of soybean after fertilization. Can J Bot 64:965–972.

——— 1988 The characteristics and fate of the soybean inner nucellus. Acta Bot Neerl 37:387–394.

——— 1989 Embryo sac development in soybean: ultrastructure of megasporogenesis and early megagametogenesis. Can J Bot 67:2841–2849.

——— 1990 Embryo sac development in soybean: cellularization and egg apparatus expansion. Can J Bot 68:2135–2147.

——— 1992 Embryo sac development in soybean: the central cell and aspects of fertilization. Am J Bot 79:1407–1417.

Folsom MW, CM Peterson 1984 Ultrastructural aspects of the mature embryo sac of soybean, *Glycine max* (L.) Merr. Bot Gaz 145:1–10.

Gori P 1987 The fine structure of the developing *Euphorbia dulcis* endosperm. Ann Bot 60:563–569.

Gunning BES, JS Pate 1974 Transfer cells. Pages 441–480 *in* AW Robards, ed. Dynamic aspects of plant ultrastructure. McGraw-Hill, Maidenhead.

Gunning BES, MW Steer 1975 Ultrastructure and biology of plant cells. Edward Arnold, London. 312 pp.

He MY, YY Zhou, ZR Xu, JS Zhang 1979 Microsporogenesis and megasporogenesis of soybean. Acta Bot Sin 21: 157–162.

Jensen WA 1969 Cotton embryogenesis: pollen tube development in the nucellus. Can J Bot 47:383–385.

——— 1974 Reproduction in flowering plants. Pages 481–

503 *in* AW Robards, ed. Dynamic aspects of plant ultrastructure. McGraw-Hill, New York.

Jensen WA, P Schulz, ME Ashton 1977 An ultrastructural study of early endosperm development and synergid changes in unfertilized cotton ovules. Planta 133:179–189.

Jones RL 1974 The structure of the lettuce endosperm. Planta 121:133–146.

Kennell JC, HT Horner 1985 Megasporogenesis and megagametogenesis in soybean, *Glycine max.* Am J Bot 72: 1553–1564.

Mansfield SG, LG Briarty 1990 Endosperm cellularization in *Arabidopsis thaliana* L. Arabidopsis Inf Serv 27:65–72.

Mares DJ, BA Stone, C Jeffrey, K Norstog 1977 Early stages in the development of wheat endosperm. II. Ultrastructural observations on cell wall formation. Aust J Bot 25:599–613.

Marinos NG 1970 Embryogenesis of the pea (*Pisum sativum*). 1. The cytological environment of the developing embryo. Protoplasma 70:261–279.

Mogensen HL 1981 Ultrastructural localization of adenosine triphosphatase in the ovules of *Saintpaulia ionantha* (Gesneriaceae) and its relation to synergid function and embryo sac nutrition. Am J Bot 68:183–194.

——— 1984 Quantitative observations on the pattern of synergid degeneration in barley. Am J Bot 71:1448–1451.

Newcomb W 1973 The development of the embryo sac of sunflower *Helianthus annuus* L. after fertilization. Can J Bot 51:879–890.

——— 1978 The development of cells in the coenocytic endosperm of the African blood lily *Haemanthus katherinae.* Can J Bot 56:483–501.

Newcomb W, LC Fowke 1973 The fine structure of the change from the free-nuclear to cellular condition in the endosperm of chickweed *Stellaria media.* Bot Gaz 134: 236–241.

Rosanoff S 1865 Uber die Kristalldrusen im Marke von *Kerria japonica* DC. und *Ricinis communis.* Bot Zeitung 23:329–330.

Russell SD, LJ Mao 1990 Patterns of embryo sac organization, synergid degeneration and cotyledon orientation in *Linum usitatissimum* L. Planta 182:52–57.

Schel JHN, H Kieft, AAM Van Lammeren 1984 Interactions between embryo and endosperm during early developmental stages of maize caryopses (*Zea mays*). Can J Bot 62:2842–2853.

Schulz P, WA Jensen 1974 *Capsella* embryogenesis: the development of the free nuclear endosperm. Protoplasma 80:183–205.

Singh AP, HL Mogensen 1976 Fine structure of early endosperm in *Quercus gambelii.* Cytologia 41:345–361.

Sumner MJ, L Van Caeseele 1989 The ultrastructure and cytochemistry of the egg apparatus of *Brassica campestris.* Can J Bot 67:177–190.

Thorne JH 1981 Morphology and ultrastructure of maternal seed tissues of soybean in relation to the import of photosynthate. Plant Physiol 67:1016–1025.

Tilton VR 1981 Ovule development in *Ornithogalum caudatum* (Liliaceae) with a review of selected papers on angiosperm reproduction. IV. Egg apparatus structure and function. New Phytol 88:505–531.

Tilton VR, LW Wilcox, RG Palmer 1984 Postfertilization wandlabrinthe and function in the central cell of soybean, *Glycine max* (L.) Merr. (Leguminosae). Bot Gaz 145:334–339.

Van Lammeren AAM 1988 Structure and function of the microtubular cytoskeleton during endosperm development in wheat: an immunofluorescence study. Protoplasma 146: 18–27.

Vijayaraghavan MR, K Prabhakar 1984 The endosperm. Pages 319–376 *in* BM Johri, ed. Embryology of angiosperms. Springer-Verlag, Berlin.

Yan H, HY Yang, WA Jensen 1991 Ultrastructure of the developing embryo sac of sunflower (*Helianthus annuus*) before and after fertilization. Can J Bot 69:191–202.

Yeung EC, ME Clutter 1978 Embryogeny of *Phaseolus coccineus:* growth and microanatomy. Protoplasma 94:19–40.